BILINGUAL PUBLISHING GROUP

Journal of Atmospheric Science Research

https://journals.bilpubgroup.com/index.php/jasr/index

ARTICLE

Evaluation of COSMO-CLM Model Parameter Sensitivity in the Study of Extreme Events across the Eastern Region of India

***Sourabh Bal*[1,2*], *Ingo Kirchner*[1]**

[1] *Institute for Meteorology, Freie Universitat, Berlin 12165, Germany*

[2] *Department of Physics, Swami Vivekananda Institute of Science and Technology, Kolkata 700145, India*

ABSTRACT

The present study aims to identify the parameters from the Consortium for Small-scale Modelling in CLimate Mode (COSMO-CLM) regional climate model that strongly controls the prediction of extreme events over West Bengal and the adjoining areas observed between 2013 to 2018. Metrics, namely Performance Score (PS) screen out the most persuasive parameter on model output. Additionally, the Performance Index (PI) measure the reliability of the model and Skill Score (SS) establishes the model performance against the reference simulation leading to the optimization of the model for a given variable. In this study, parameter screening for four output variables such as 2m-temperature, surface latent heat flux, precipitation and cloud cover of COSMO-CLM is accomplished. For heat wave simulations, 2m-temperature and surface latent heat flux are explored whereas cloud cover and precipitation are examined for extreme rainfall events. A total of 25 adjustable parameters representing the following parameterization schemes: turbulence, land surface process, microphysics, convection, radiation and soil. Out of the six parameterization schemes, the scaling factor of the laminar boundary layer for heat (rlam_heat) and the ratio of laminar scaling factors for heat over sea and land (rat_sea) from the land surface process is sensitive to SLH, TP. The exponent to get the effective surface area (e_surf) from the land surface has a large impact on 2m-temperature. A few parameters from microphysics (cloud ice threshold for auto conversion), convection (mean entrainment rate for shallow convection) and radiation (parameter for computing the amount of cloud cover in saturated conditions) play a significant role in producing TP, and TCC fields. It is evident from the results that the parameter sensitivities on model performance depend on the choice of the meteorological field. Furthermore, in almost all input model parameters, the model performance reveals the opposite character in different domains for a given meteorological field.

Keywords: India; Climate models; Model sensitivity; COSMO-CLM; Model evaluation

*CORRESPONDING AUTHOR:

Sourabh Bal, Institute for Meteorology, Freie Universitat, Berlin 12165, Germany; Department of Physics, Swami Vivekananda Institute of Science and Technology, Kolkata 700145, India; Email: sourabhbal@zedat.fu-berlin.de

ARTICLE INFO

Received: 26 January 2024 | Revised: 21 March 2024 | Accepted: 17 April 2024 | Published Online: 25 April 2024

DOI: https://doi.org/10.30564/jasr.v7i2.6226

CITATION

Bal, S., Kirchner, I., 2024. Evaluation of COSMO-CLM Model Parameter Sensitivity in the Study of Extreme Events across the Eastern Region of India. Journal of Atmospheric Science Research. 7(2): 19–40. DOI: https://doi.org/10.30564/jasr.v7i2.6226

1. Introduction

In recent years, India has experienced several extreme weather events that have caused human casualties, infrastructure damage, and economic losses. These events include intense and frequent heat waves, an increase in extreme rainfall events, and storms [1–6]. Coastal areas of India are susceptible to tropical cyclones that bring heavy rainfall and high-speed winds originating from the Arabian Sea and the Bay of Bengal [7–9]. For example, two severe cyclones, both in the month of May, Amphan in 2020 and Yaas in 2021 made landfall along the coast of Bengal and Orissa, affecting the lives of millions with a total economic loss of more than 16 billion US dollars [10–16]. In the recent past, similar extreme events caused by heavy rainfall in other sectors of India damaged crops and disrupted lives. Numerous studies have indicated that India and its coastal regions are at risk of experiencing severe weather conditions in the near future due to climate change and human-induced warming [6,7,17–22]. It is, therefore, essential to have accurate predictions of these weather events well in advance in order to minimize the damage caused by such extreme events.

Climate models play a very important role in reproducing present climate and projecting future climate including climate extremes. Global climate models can resolve large-scale features such as circulation however often fail to arrest fine-scale processes for their poor spatial resolution [23,24]. On the other hand, regional climate models have an added advantage, particularly improved spatial resolution to respond to small-scale processes in simulating extreme events [4]. Compared to general circulation models, regional climate models enhance the quality of the model output and also add detailed information at a regional scale, particularly in predicting regional extreme weather events [20,25,26]. During the last decades, regional models have significantly upgraded in terms of resolution that can describe more detailed spatial and temporal distribution of climate variables. Even model evolutions were carried out with superior representations of the atmosphere and timely forecasts of an atmospheric system [26,27].

Standardizing climate models remains certainly an essential measure before future prediction by sophisticated methods such as data assimilation, and model output analysis. The competence of climate models is determined against observational datasets to point out model deficits which arise from various model assumptions associated with model uncertainties [28–30].

The COSMO-CLM (Consortium for Small-scale Modelling in CLimate Mode) was ingeniously developed for European Climate. Later, with the growth of other mesoscale climate models, the transformation of COSMO-CLM model has progressed to the next generation region climate model in terms of model architecture tested over multiple climate regions of the globe. The capacity of COSMO-CLM model depends mainly on three elements. The first two elements are related to initial and boundary conditions and presumed physics, coupled with the basic representation of sub-grid-scale processes known as parameterization [31,32]. The model generally includes multiple numerical schemes parameterizing various physical processes namely, surface-atmosphere interaction, cloud physics, turbulences, convection, and radiation that consist of several unconfined parameters [33]. The third element influencing COSMO-CLM performance is to quantify the model parameters. These model parameters account for a significant source of uncertainties in climate model simulations. Numerous research papers illustrate the gravity of the parameter uncertainty in model simulation after perturbing single or several parameters within the conceivable range [34–36]. This approach is commonly known as sensitivity analysis to identify the most important parameters in a model. Numerous techniques involved in the calibration of climate models have evolved in recent years such as Monte Carlo integrations, ensemble Kalman filters etc [37]. Some of these methods are not readily implemented in high-resolution climate models to investigate the parameter space because a classically large number of simulations are to be conducted [38]. This challenge can be resolved by identifying the most influencing parameter on model output and tuning these parameters so thereby model performance is optimized [28,33,34,39]. The COSMO-CLM parameter

sensitivity for the Coordinated Regional Climate Downscaling Experiment (CORDEX) European domain was tested by Bellprat et al., (2012) [38, 40] with multiple simulation periods, additionally examining the interplay between two parameters at a time, modifying their values in their proportionate extent. Finally, led to deducing an optimal model configuration for the European domain following the second-order polynomial metamodel proposed by Neelin et al., (2010) [41]. With a similar approach, the flexibility of the determined model configuration to other regions was successfully presented [25,34,42–45].

Numerous sensitivity analysis studies on parameters of community-based Numerical Weather Prediction systems with respect to different parameterization schemes to improve the prediction of extreme events particularly over the Greater Beijing area [46,47], in the Indian region [48], over the Bay of Bengal [8]. In recent work, the COSMO-CLM parameter sensitivity for the CORDEX Central Asian domain was examined from a set of 1-year-long simulations and concluded that the sensitive parameter identified is different than the one observed in Europe. Their results also suggest that only a subset of model parameters present brings improvement in model performance for different parameter values [39].

To our best knowledge, no evaluation study has been made using COSMO-CLM in simulating extreme weather events, particularly in the eastern Indian sector. In this paper, the COSMO-CLM parameter sensitivity was performed, after selecting eleven extreme events from the eastern part of India testing a range of inputs for an extensive number of model parameters. These extreme events were classified into two types: heat wave events, heavy rainfall events. The primary aim of this work is to identify the most sensitive model parameters for the study domain in favour of having the ideal model configuration. Simultaneously, from the model skill score for the study region, the probable cause of shortfalls over different sub-areas with alike climate environments is associated with the most appropriate parameters in each area. The present work constitutes four heat wave events, and seven heavy rainfall events. For heat wave events, we evaluated the sensitivity of the model parameters on 2m-temperature and surface latent heat flux. The sensitivity of the model by the parameters due to heavy precipitation events was explored using precipitation and cloud cover.

The article is structured in the following manner: Section 2 provides a general description of the model setup for the COSMO-CLM domain. Section 3 explains the simulation events and the reanalysis datasets used. Section 4 outlines the methodology and the evaluation tools. In section 5, the results are presented and discussed. The final section summarizes the conclusions and discusses future research and development related to the presented findings.

2. Model and design of experiments

The COSMO-CLM, a three-dimensional non-hydrostatic regional model was optimized using parameter sensitivity analysis over eastern India and adopted for all the simulations presented in this work [49]. It was developed by the German Weather Service (DWD) and CLM Community [50]. The COSMO-CLM version used in this work is COSMO-CLM 5.0_clm6 [51]. A full description of the COSMO model physics, dynamics and parameterization is available at http://www.clm-community.eu [52]. The initial boundary conditions for the COSMO-CLM were obtained from the European Centre for Medium-Range Weather Forecasts (ECMWF) reanalysis data sets with 6-hourly data at 0.5° × 0.5° resolution [53]. The model configuration for all the simulations were performed over the domain (81.25°–94.64° E, 15.87°–27.76° N) shown as a red box in **Figure 1** employing a 0.10° spatial resolution with a third-order Runge-Kutta scheme. The time step for integration was 150 for the computational domain. The computational domain comprises 120 grid points in both the north-south direction and east-west direction. The model produces output with a 3-hour frequency. The Tiedtke scheme was used for the convection parameterization [54]. The number of atmospheric vertical levels was fixed at 40. The representation of soil moisture was performed using a 9-layer soil module, TERRA-ML, having a depth

of 11.5 m. The default Tanre aerosol distribution was adopted, it uses constant aerosol values for desert, sea land and urban areas [55]. COSMO-CLM has a wide application starting from past, present and future studies and can run at different spatial scales and varied climate zones [25, 26, 28-30, 39, 42, 43, 45, 56-61].

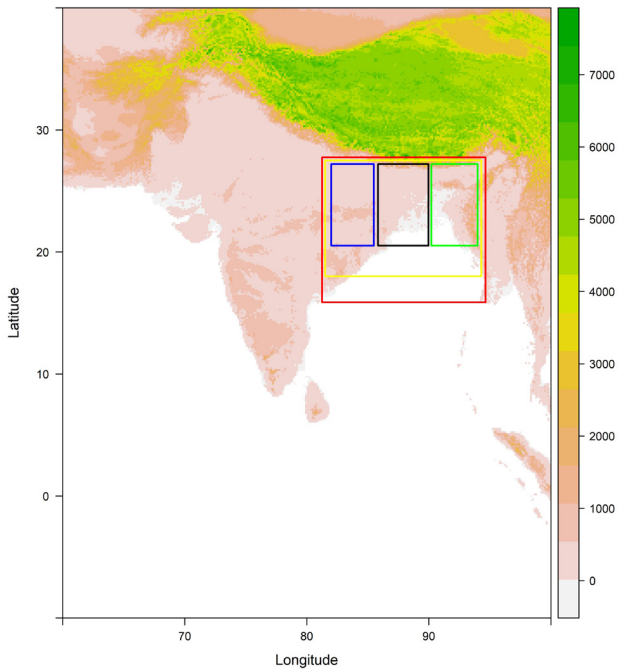

Figure 1. The computational domain (WD) in red and the orography of the Indian region (in m) are considered. The four sub-regions are highlighted: ID (inner domain in yellow); LWB (Left of West Bengal i.e Bihar and Orissa in blue); WB (West Bengal in black); RWB (Right of West of West Bengal in green).

The study focuses on extreme weather events that occurred between 2013 and 2018 in West Bengal and its neighboring regions. The researchers identified the key date for each of the extreme events and used COSMO-CLM to simulate each event for an 11-day, including 5 days before and after the key date, at 3-hour intervals. Accordingly, nine events were identified for the evaluation of the impact of parametric uncertainty on the 11-day forecasts. We identified 25 adjustable tunable parameters from five parameterizations such as sub-grid scale turbulence, land-surface parameterization, microphysics, radiation, convection, and soil that may influence 2m-temperature, surface latent heat flux, precipitation and cloud cover. **Table 1** presents a complete list of physical schemes along with their parameters, physical meanings, and allowable ranges. To perform a sensitivity analysis, simulations were executed on the COSMO-CLM model, using a comprehensive set of values assigned to these parameters. The examined model parameters spread across plausible maximum, minimum and intermediate values and generate 64 parameter samples out of 25 tunable parameters. When the value of each tunable parameter is set at default, then the simulation is referred to as a reference simulation. These parameter sets were assigned in the COSMO-CLM model, and a total of 11 × (64 + 1) = 715 simulations were performed across eleven extreme events.

3. Simulation events, COSMO-CLM output variables, and observational data

Commonly, hurricanes, tornadoes and thunderstorms are identified as extreme weather events. Extreme weather also includes severe unexpectable weather such as heat waves, cold waves and floods. However, cold waves are not conventional in the study region. A list of eleven extreme weather events was prepared from different media sources reporting the occurrence of these events in West Bengal in the period from 2013 to 2018 [62]. The enlisted extreme events are presented in **Table 2** from a variety of extreme categories such as heavy rain events and heat waves days with their start and end dates. From the list of extreme events **Table 2** from a variety of extreme categories such as heavy rain and heat wave with their start and end dates. From the list of extreme events (**Table 2**), four events were counted as heat wave events experienced during March, April and May labelled as exp01 to exp04. In the same list, five heavy rain events were categorized, occurring in June, July, August and October designated as exp05 to exp11. The output variables from each simulations had to be validated with the reanalysis data to verify the reliability of the simulations. In this study, the fifth-generation reanalysis popularly known as ERA-5, released by ECMWF was employed for model evaluation [63]. ERA-5 reanalysis is an upgraded version of Era-Interim and it is better than Modern Era Representative Analysis for Research and Applications

Table 1. List of tuning parameters for different parameterization schemes and respective ranges of examined model parameter values with default model configuration are rendered in bold.

Parameter	Description	Values
Turbulence		
tkhmin	minimal diffusion coefficients for heat	(0, **0.4**, 1, 2)
tkmmin	minimal diffusion coefficients for momentum	(0, **0.4**, 1, 2)
tur_len	maximal turbulent length scale	(100, **500**, 1000)
d_heat	factor for turbulent heat dissipation	(12, **10.1**, 15)
d_mom	factor for turbulent momentum dissipation	(12, 15, **16.6**)
c_diff	factor for turbulent diffusion of TKE	(0.01, **0.2**, 10)
q_crit	critical value for normalized oversaturation	(1, **4**, 7, 10)
clc_diag	cloud cover at saturation in statistical cloud diagnostic	(0.2, **0.5**, 0.8)
Land Surface		
rlam_heat	scaling factor of the laminar boundary layer for heat	(0.1, **1**, 3, 5, 10)
rat_sea	ratio of laminar scaling factors for heat over sea and land	(1, 10, **20**, 50, 100)
rat_can	ratio of canopy height over z0m	(0,**1**, 10)
rat_lam	ratio of laminar scaling factors for vapour and heat	(0.1, **1**, 10)
c_sea	surface area density of the waves over sea [1/m]	(1, **1.5**, 5, 10)
c_lnd	surface area density of the roughness elements over land	(1, **2**, 10)
z0m_dia	roughness length of a typical synoptic station	(0.001, **0.2**, 10)
pat_len	length scale of subscale surface patterns over land	(10, 100, **500**, 1000)
e_surf	exponent to get the effective surface area	(0.1, **1**, 3)
Convection		
entr_sc	mean entrainment rate for shallow convection	(5e-5, 1e-4, **3e-4**, 1e-3, 2e-3)
Microphysics		
cloud_num	cloud droplet number concentration	(5e + 7, **5e + 8**, 1e + 9)
qi0	cloud ice threshold for autoconversion	(**0**, 0.00001, 0.0001, 0.001, 0.01)
v0snow	factor for fall velocity snow	(10, 15, **25**)
Radiation		
uc1	parameter for computing amount of cloud cover in saturated conditions	(0.2, 0.5, 0.625, **0.8**)
radfac	fraction of cloud water/ice used in radiation scheme	(0.3, **0.5**, 0.9)
Soil		
soilhyd	multiplication factor for hydraulic conductivity and diffusivity	(**1**,1.62,6)
fac_rootdp2	uniform factor for the root depth field	(0.5,**1**,1.5)

(MERRA) and Era-Interim in terms of horizontal resolution [64,65]. Simulated 2m-temperature (T2M) and surface latent heat flux (SLHF) were validated against ERA-5 gridded data sets for heat wave events. Precipitation (TP), and cloud cover (TCC) from the same reanalysis source have been used to validate heavy rainfall events produced by the model. The reanalysis data set provides 3-hourly daily data with 0.25° × 0.25° spatial resolution. Simulated precipitation (TP) is validated against Integrated

Multi-satellitE Retrievals for Global Precipitation Measurement (IMERG) dataset [66]. The IMERG data is a multi-satellite precipitation estimate with gauge calibration which is recommended for study. The IMERG data is available roughly at 10 km by 10 km resolution with 30-minute latency. Since the model resolution is close to the validation data resolution, it results in very little or no loss of data after re-griding takes place. The variables which are assessed for evaluation were transformed into their respective units uniformly. 2m-temperature, surface latent heat flux, precipitation and cloud cover were measured in Kelvin, Wattm^{-2} mms^{-1} and fraction respectively.

Table 2. List of selected extreme events simulated by COSMO-CLM in this study with the start and end dates.

Event	Start date	End date	Event type
exp01	2014–04–20	2014–04–30	Heat Wave
exp02	2014–05–16	2014–05–26	Heat Wave
exp03	2015–05–18	2015–05–28	Heat Wave
exp04	2018–06–13	2018–06–23	Heat Wave
exp05	2018–06–19	2018–06–29	Heavy Rain
exp06	2015–07–23	2015–08–02	Heavy Rain
exp07	2013–08–15	2013–08–25	Heavy Rain
exp08	2014–06–27	2014–07–07	Heavy Rain
exp09	2015–07–05	2015–07–15	Heavy Rain
exp10	2014-10-05	2014-10-15	Heavy Rain
exp11	2013-10-08	2013-10-18	Heavy Rain

Source: Asis et al [62].

4. Methodology

Evaluation of the model parameter uncertainties is executed by a wide range of methodologies which is generally termed as sensitive analysis. The initial steps of sensitive analysis include a selection of climate models and the corresponding best set of physical schemes, followed by recognizing the notable input parameters and associated ranges. **Table 1** presents the details of the selection of the model parameters and their input ranges. The last steps consist of calculating metrics from an established theory analysing the model outputs and quantifying the sensitivity of selected parameters.

There are numerous metrics derived from several established methods to endorse the performance of the model in connection with considered model parameters. The present method is adopted in this study to distinguish the sensitive parameters from the insensitive ones. Furthermore, it also captures the model performance concerning reference simulation as a function of variables and regions. First, we present the sensitive analysis by the Performance Index (PI) metric, which has been deduced from the Climate Performance Index based on scaled root mean square error (RMSE) [39, 40, 67–70] presented in equation (1). RMSE is normalized using the standard deviation of observations, averaged over the climate variables at a given region r where h is the dimension of time and e represents a particular extreme event.

$$PI = \frac{1}{n_v \times n_r \times n_h \times n_e} \sum v \sum r \sum h \sum e \left[\frac{\sqrt{(F_{v,r,h,e} - O_{v,r,h,e})^2}}{\sigma_{O_{v,r,h,e}}} \right] \quad (1)$$

Where n_v corresponds to the examined number of climate variables, n_r is the number of domains and n_h represents the number of time intervals in n_e several events. For a given experiment, COSMO-CLM field value $F_{v,r,h,e}$ is for a variable v, over the region at a given time h against the observation $O_{v,r,h,e}$ for the same variable v, same region r and at the same time h. σ_O is the standard deviation estimated from the observed data. We have considered nine extreme events from 2013 to 2018 in eastern India. Each event simulates for 11 days and stores output at 3 h intervals. PI is calculated for 2TM and SLH from exp01 to exp04 and from exp05 to exp09, CC and TP were used, together on four inner sub-domains in addition to the simulation domain shown in **Figure 1**. Detailed definition of each domain is as follows: (a) Simulation domain (WD): 81.25°–94.64° E, 15.87°–27.76° N, (b) Inner Domain (ID): 81.50°–94.30° E, 18°–27.50° N, (c) Left West of West Bengal (LWB): 82°–85.50° E, 20.52°–27.20° N, (d) West Bengal (WB): 85.83°–89.96° E, 20.52°–27.20° N, (e) Right of West Bengal (RWB): 90.2°–94° E, 20.52°–27.20° N. Therefore, n_v=4, n_r=5, n_h=88. PI is also computed for each variable separately.

PI measures the reliability of the model. The

lower value of PI implies good performance by the model and vice-versa. With the estimated PI, Performance Score (PS) is derived from equation (2), for each set of parameters.

$$PS = e^{(-0.5PI^2)} \tag{2}$$

Basically, PI allows us to quantify model parameter uncertainty, while PS is used as an estimate of the model sensitivity to each single tested parameter.

The PS values are presented and smoothened by quadratic regression for a set of model parameters highlighting the model sensitivity for that specific parameter considering each variable separately.

In the next step, model parameter uncertainties for the study domain and sub-domains are investigated. Then, the variable and region dependent PI is expressed with respect to the one of the reference simulations using a skill score (SS) defined in equation (3) as

$$SS = \left(1 - \frac{PI_{sim}}{PI_{ref}}\right) \tag{3}$$

Here PI_{sim} and PI_{ref} stands for PI value of a simulation for a given variable and region and PI value for default model configuration respectively.

The negative SS values indicate underestimation of 2m-temperature, surface latent heat flux, precipitation, and cloud cover for a given domain by the model at a given set of parameters (simulation) than the reference simulation (parameters set at default values). Positive values show better model performance and 1 infers the best achievable score. Out of all the simulations, the simulation with the best skill score is identified as the simulation with optimum parameters.

5. Results

5.1 Parameter sensitivity analysis

2m-temperature, surface latent heat flux was used to evaluate the sensitivity of the model parameters for the extreme heat wave events enlisted in **Table 2**. For heavy rainfall events, total precipitation and cloud cover were considered. Initially, PS was calculated for each variable influenced by the tuning parameters. The sensitivity plots with 2m-temperature and surface latent heat flux are presented in **Figure 2**. In the same plot, PS with each considered tuning parameters for heavy rainfall events influencing precipitation and cloud cover is plotted in **Figure 2**. In each subplot, the x-axis represents the values of the selected parameter and y-axis contains the PS value corresponding to each parameter value. The default value of each parameter in every subplot is highlighted in red. 2m-temperature, surface latent heat flux is depicted in a square, asterisk respectively for all the subplots. The most sensitive parameters for the study region in simulating 2m-temperature and surface latent heat flux are exponent to get the effective surface area **(e_surf)**. The next set of parameters which have an appreciable influence on latent heat flux by PS is the scaling factor of the laminar boundary layer for heat **(rlam_heat)**, the ratio of laminar scaling factors for heat over sea and land **(rat_sea)**. No parameters from turbulence, convection, radiation and soil scheme influence PS in simulating 2m-temperature and surface latent heat flux. In **Figure 2**, precipitation and cloud cover are depicted in filled diamonds and filled square respectively for all the subplots. For both precipitation and cloud cover, the most noteworthy variation in PS is observed for cloud ice threshold for auto conversion **(qi0)** from the microphysics process. It is also observed that for qi0, the changes in PS in simulating cloud cover, show reverse character to precipitation. The second set of parameters which strongly influence the precipitation simulation is **rlam_heat**, and **rat_sea** from the surface interaction process. Russo et al., (2020) [39] in their study of the South Asian CORDEX region identified the same set of parameters. The mean entrainment rate for shallow convection **(entr_sc)** from the convection scheme and parameter for computing the amount of cloud cover in saturated conditions **(uc1)** from the radiation scheme influence the variation of PS in computing the cloud cover. There is no significant change in PS for extreme rainfall events and cyclones for other parameters representing different processes. On the whole, it is notable that the value of PS is lowest in precipitation followed by cloud cover, 2m-temperature and surface latent heat flux.

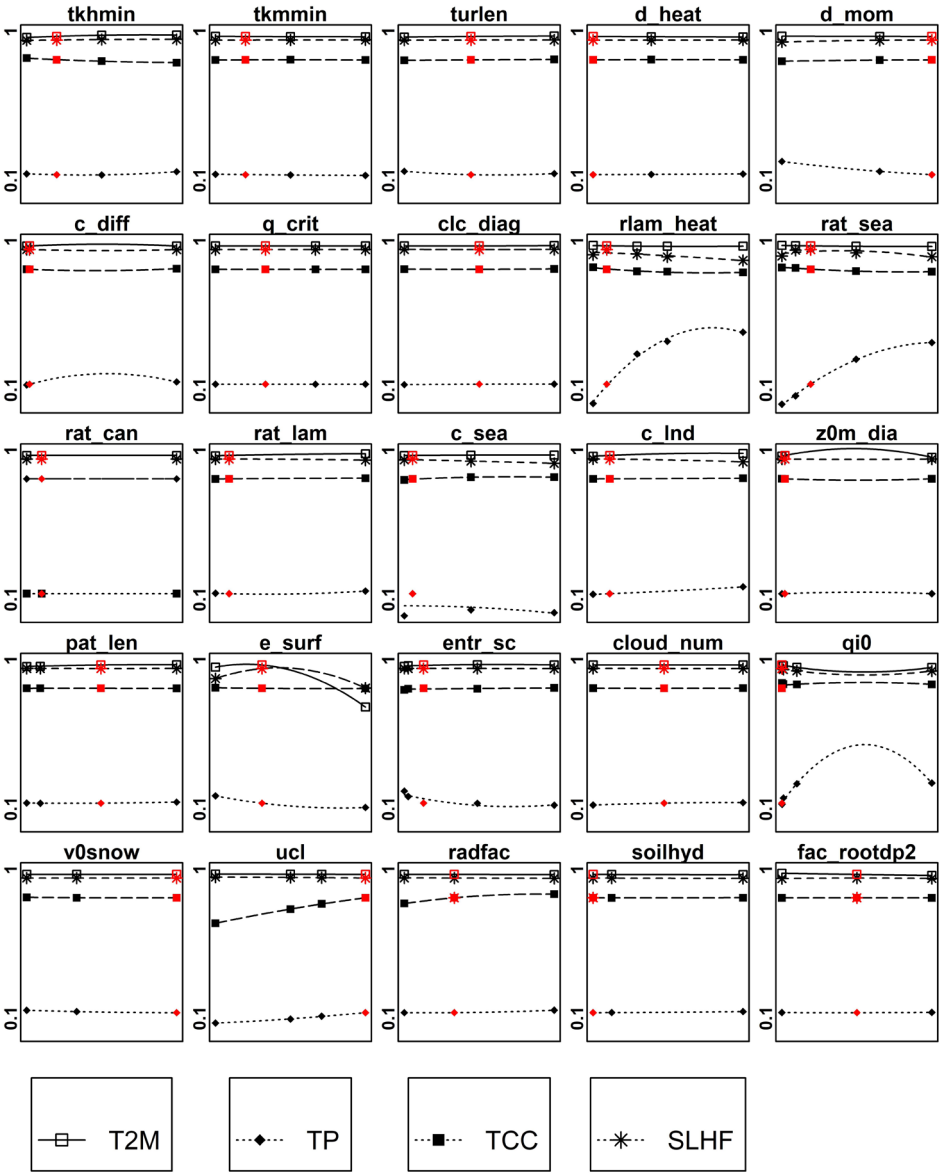

Figure 2. Performance Score (PS) are computed separately from exp01 to exp04 (Table 2) for 2m-temperature (T2M: solid line with square), surface latent heat flux (SLHF: dotted line with asterisk) for all the considered parameter values over the entire study region in heat wave events. From exp5 to exp11 (Table 2) which includes heavy rain events, PS are computed separately for total precipitation (TP: dotted line with filled diamond) and cloud cover (TCC: dotted line with filled square) over the entire domain of study. In each subplot, the x-axis represents the values of the selected parameter and y-axis contains the PS value corresponding to each parameter value. The red points show the calculated PS value for the default model configuration.

PS was also calculated for all three variables together for each parameter value illustrated in **Figure 3**. The most sensitive parameters which strongly influence the model output for all the considered atmospheric variables are the members of the land surface interaction scheme and microphysics scheme. The three parameters from the surface interaction scheme are the surface area density of the waves over the sea [1/m] **(c_sea)**, the scaling factor of the laminar boundary layer for heat **(rlam_heat)**, the ratio of laminar scaling factors for heat over sea and land **(rat_sea)**, exponent to get the effective surface area **(e_surf)** and cloud ice threshold for autoconversion (qi0) from microphysics scheme. There are model parameters which show small or zero changes in the combined PS for all the variables can be justified that the variation of PS for different variables counterbalance mutually.

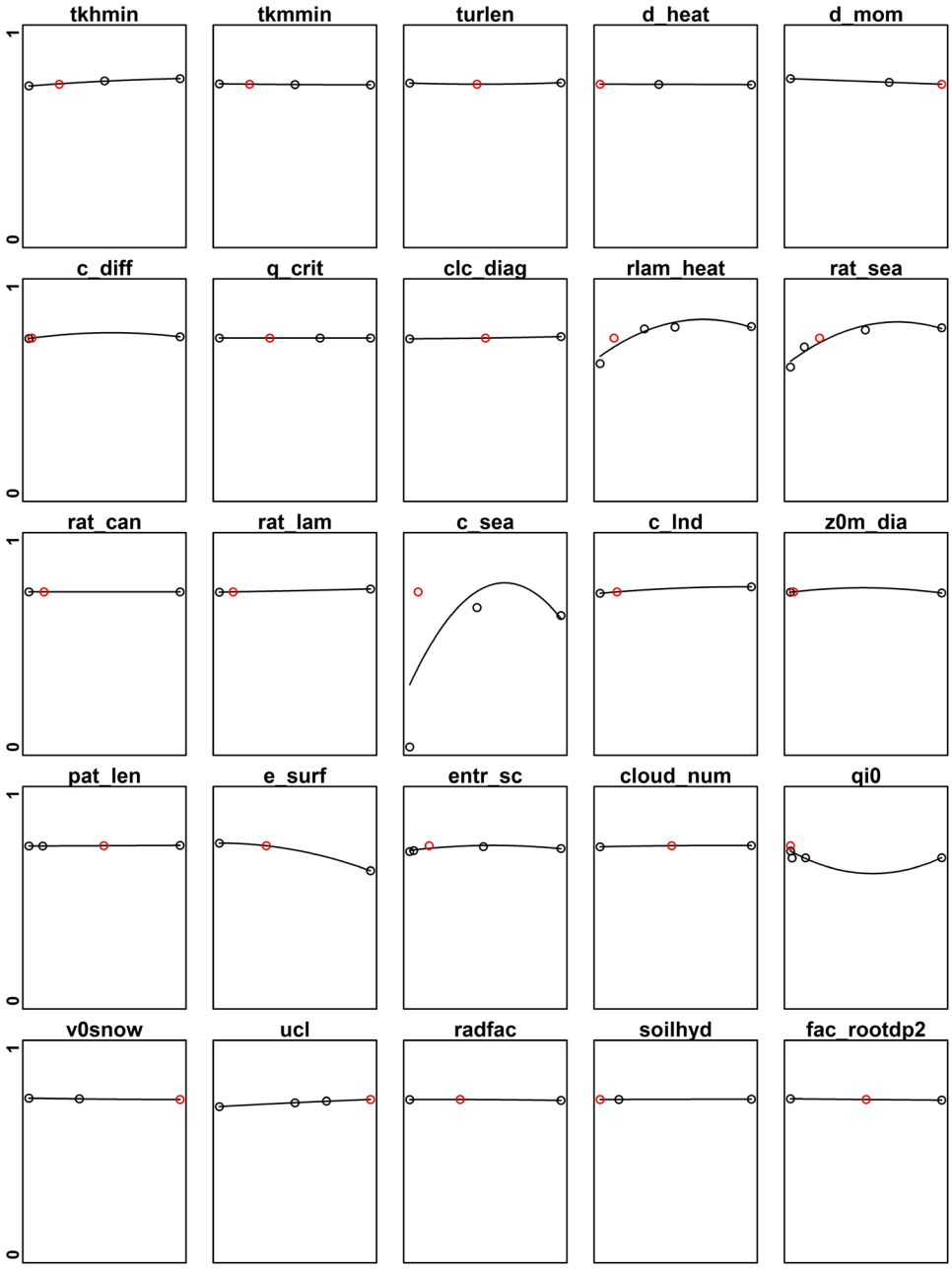

Figure 3. The red points show the calculated PS value for the default model configuration. Considering all the variables together (T2M, SLHF, TP, TCC), Performance Score (PS) are computed from heat wave events and heavy rain events (exp01 to exp11 explained in Table 2) for all the considered model parameters values over the entire domain of study. In each subplot, the x-axis represents the values of the selected parameter and y-axis contains the PS value corresponding to each parameter value. The red points show the calculated PS value for default model configuration.

5.2 Model performances in different domains

After identifying the sensitive model parameters, the second objective of this work is to investigate the model parameter uncertainties to determine the most relevant process involved in each simulation and assess to which degree it is possible to improve model performance for the considered variables by properly setting values. Immediately after the most sensitive model parameters for the study area are detected, the ability of the model is recognized for each variable and sub-region as a function of PI and SS. PI estimated for reference simulation for a given region is plotted in the vertical axis against the computational

domain and each evaluation domain in the horizontal axis. The lower PI signifies better performance by the model. PI value for each domain for T2M is shown in **Figure 4a**. For T2M, PI increases from a larger domain size to sub-domains suggesting divergence between the observation and the reference simulation and underestimation of model execution during the transition to a smaller domain size. The value of PI in each domain is high for TP (**Figure 7a**) and TCC (**Figure 6a)** indicating poor performance compared to T2M (**Figure 4a**) and SLHF (**Figure 5a**). As the magnitude of the PI value suggests the performance of the model, therefore model performs best in simulating T2M (**Figure 4a**) followed by SLHF (**Figure 5a**), TCC (**Figure 7a**) and TP (**Figure 7a**).

In the final stage of the analysis, the PI for each simulation corresponding to the set of parameters was estimated against the reference simulation and expressed as SS. The SS for each experiment and domain is illustrated in **Figure 4b**, **Figure 5b, Figure 6b**, and **Figure 7b** for T2M, SLHF, TCC, TP respectively as a heatmap with a red shade indicating inferior performance and a green shade implies better performance. Changes in SS for T2M (**Figure 4b**) suggest that there is no substantial change by the model against the reference simulation for all the experiments and parameters either in the direction of improvement or worsening except for **e_surf**. The largest negative SS change is observed for the maximum **e_surf** value followed by **qi0**. However, the best performance by the model in LWB domain is noted at the minimum value of **e_surf**. Hence, there is a chance to improve the model performance by tuning the **e_surf** parameter. Positive SS for T2M is estimated over the entire study region by high minima diffusion coefficients for heat (tkhmin), the high surface area density of the roughness elements over land (c_lnd) and low uniform factor for root depth field (fac_rootdp2).

In simulating SLHF (**Figure 5b**), the land surface interaction scheme plays the most important role. The potential of the model after tuning with parameters does not conduct well for all domains consistently against reference simulation. Model performance could be improved for **rlam_heat** and **rat_sea, e_surf** at its high value whereas the lower limit of **c_sea** might bring the model output in better agreement with respect to reference simulation. It is to be noted that the sensitive parameters such as **rlam_heat**, **rat_sea**, **e_surf** and **c_sea** were successful to remain coherent for subdomains but their performance in the whole domain is poor.

Out of the 64 parameter sets, changes in SS show that most parameters from convection, microphysics and radiation schemes strongly influence the prediction of TCC. Positive SS changes are noted for **cloud_num** values against its default in almost all domains (**Figure 6b**). The SS changes are notably negative for **uc1**, **qi0**, and **entr_sc** proving that the model performance is underestimated compared to the model parameter at default values. High **entr_sc** and **uc1** could influence the model to perform better confirmed by the changes in negative SS. The remaining parameters have a minimal contribution to simulating TCC.

Parameters from the surface parameterization scheme also play a vital role in simulating TP. Higher **rlam_heat**, **rat_sea** values and lower **c_sea** values against the default values have the potential to drive the model to perform better in estimating TP against the reference simulation (**Figure 7b**). The parameter for computing the amount of cloud cover in saturated conditions **(uc1)** from the radiation scheme, **qi0** from microphysics, mean entrainment rate for shallow convection **(entr_sc)** from the convection scheme and factor for turbulent momentum dissipation **(d_mom)** from turbulence scheme are the next set sensitive parameters to simulate TP by the model as evident from the changes in SS against the default values (**Figure 7b**). Two recent studies identify the model parameter defined as the multiplier for entrainment flux rate as the most significant to reproduce precipitation in high-intensity precipitation events by Weather Research Forecasting (WRF) model [46, 48, 71–73].

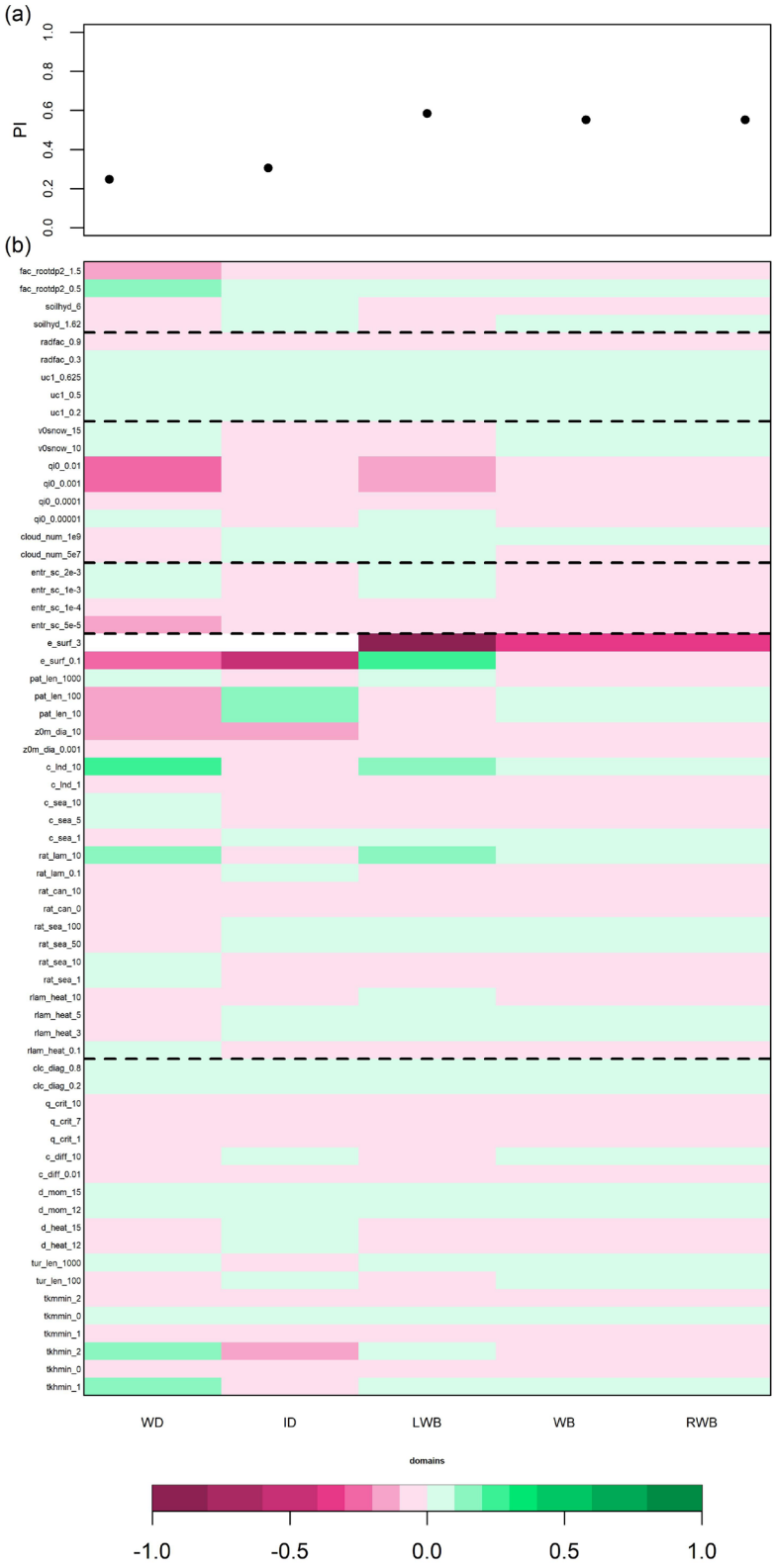

Figure 4. (a) The calculated PI for 2m-temperature (T2M) from heat wave events (exp01 to exp04) with default parameter values over the study region and four sub-regions **(b)** Variation in Skill Score (SS) in each 64 simulations (with different parameter values shown in Table 1) calculated against the reference simulation (parameter values in bold shown in Table 1) for T2M as a function of domains. Positive (Negative) SS values in green (purple) highlight better (worse) agreement with observations with respect to the reference simulation.

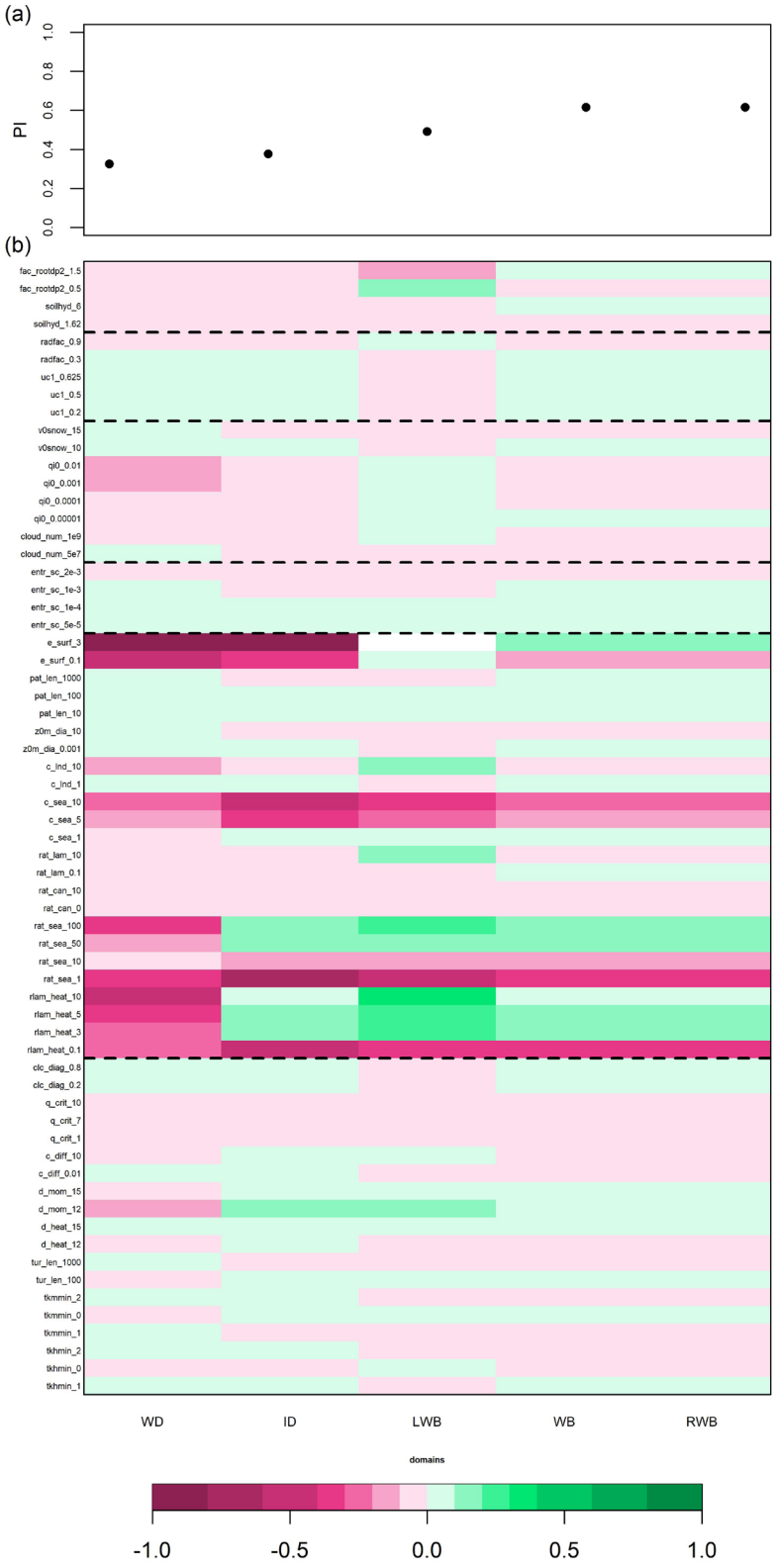

Figure 5. (a) The calculated PI for surface latent heat flux (SLHF) from heat wave events (exp01 to exp04) with default parameter values over the study region and four sub-regions **(b)** Variation in Skill Score (SS) in each 64 simulations (with different parameter values shown in Table 1) calculated against the reference simulation (parameter values in bold shown in Table 1) for SLHF as a function of domains. Positive (Negative) SS values in green (purple) highlight better (worse) agreement with observations with respect to the reference simulation.

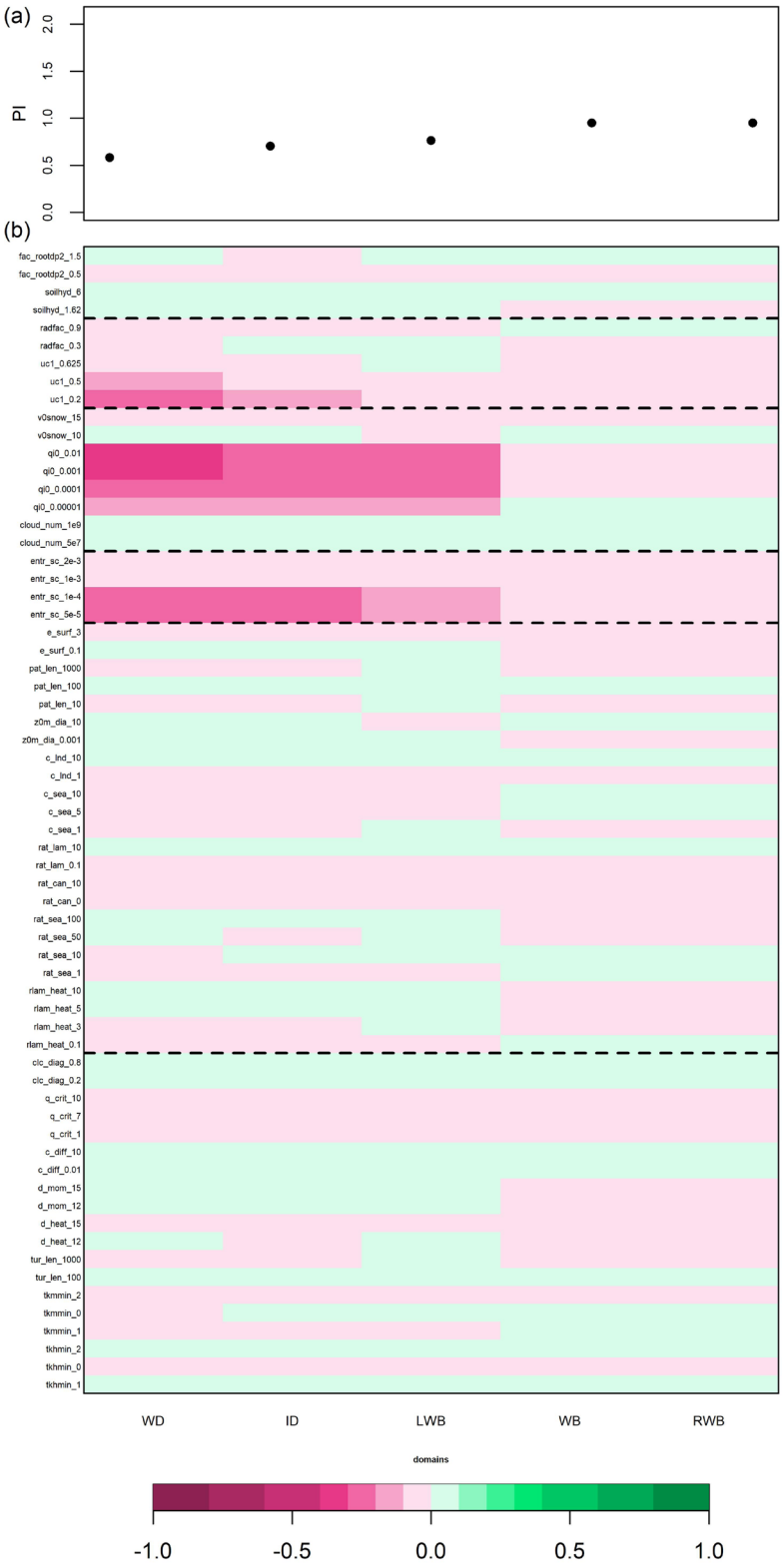

Figure 6. (a) The calculated PI for cloud cover (TCC) from heavy rain events (exp05 to exp11) with default parameter values over the study region and four sub-regions **(b)** Variation in Skill Score (SS) in each 64 simulations (with different parameter values shown in Table 1) calculated against the reference simulation (parameter values in bold shown in Table 1) for TCC as a function of domains. Positive (Negative) SS values in green (purple) indicate better (worse) agreement with observations with respect to the reference simulation.

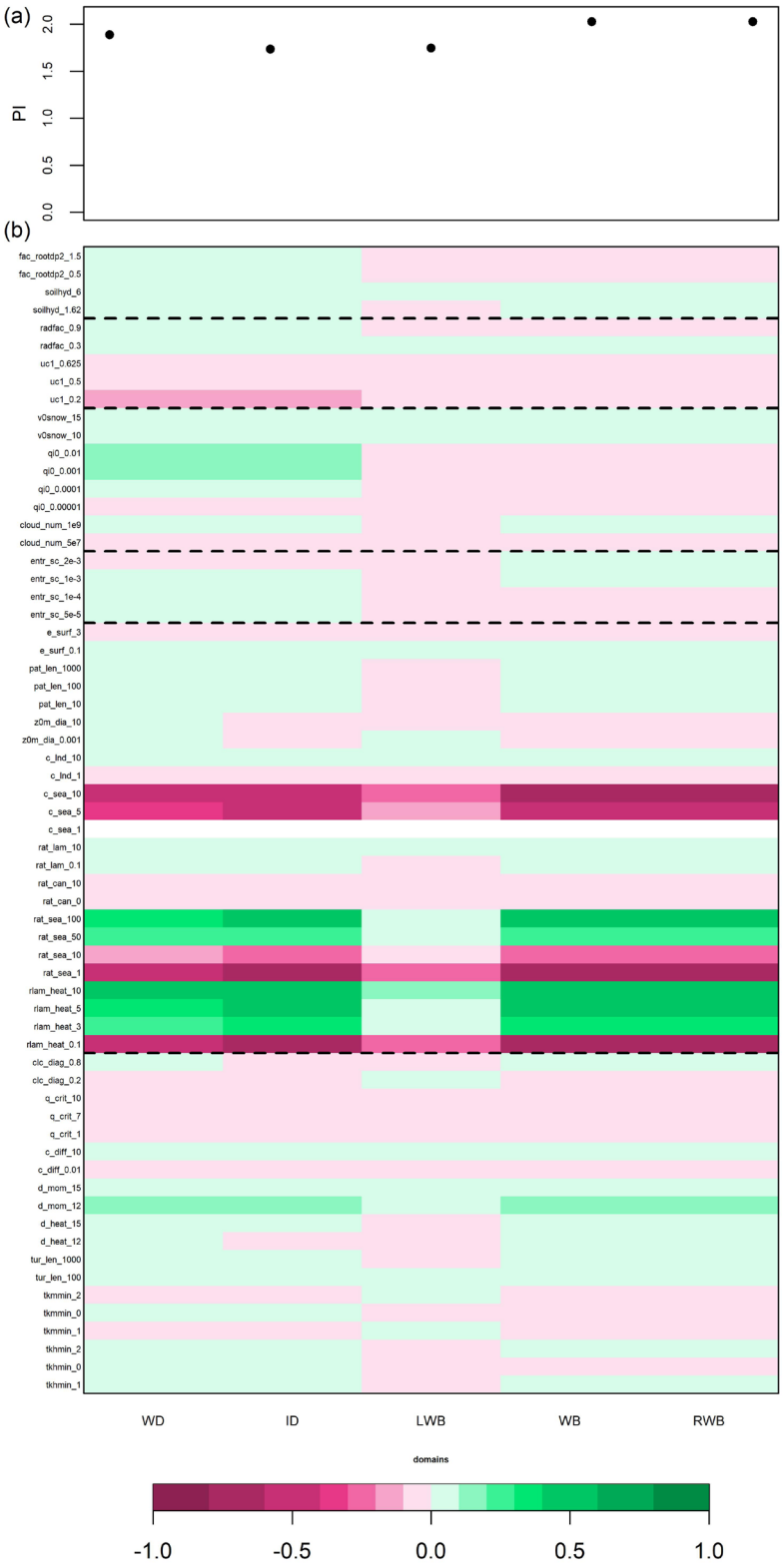

Figure 7. (a) The calculated PI for total precipitation (TP) from heavy rain events (exp05 to exp11) with default parameter values over the study region and four sub-regions **(b)** Variation in Skill Score (SS) in each 64 simulations (with different parameter values shown in Table 1) calculated against the reference simulation (parameter values in bold shown in Table 1) for TP as a function of domains. Positive (Negative) SS values in green (purple) indicate better (worse) agreement with observations with respect to the reference simulation.

5.3 Physical interpretation of parameter sensitivity

The results obtained by PS suggest that only a few parameters strongly influence the combined meteorological variables under consideration. These parameters are **rlam_heat**, **rat_sea, c_sea**, **e_surf**, **qi0**. Additionally, parameters which have some effect on model output are **tkhmin, entr_sc** and **uc1.**

In the land surface and turbulence scheme, the sensitive parameters are related to heat flux and moisture transport over land and sea. The parameter, **tkhmin** controls the minimum limit for the turbulence for heat and moisture. The value of **tkhmin** remains significant till the turbulent diffusion coefficients are less. Increment in **tkhmin** will sustain the turbulent kinetic energy, thereby mechanically increasing the mixing with highly stable stratification and resulting increase in temperature as well as an overestimation of cloud formation [74]. Parameter **rlam_heat** accounts for the heat resistance length of the laminar layer over land and sea. Laminar resistance is added by **rat_sea**, laminar resistance over sea further increases the resistance of the laminar layer. Greater **rlam_heat** value contributes to lower heat transport between the surface and the lower atmosphere, leading to a lowering of 2m-temperature. Consequently, an increase in laminar resistance reduces the moisture transport thereby reducing the total precipitation. In the cold surface condition, an increase in **rlam_heat** decreases the heat flux from the atmosphere to the surface and thereby drives to a higher 2m-temperature [75, 76]. The exchange of heat, moisture and momentum between the surface and the lower atmosphere is also shaped by the surface area density of the waves over the sea (**c_sea**) and exponent to get the effective surface (**e_surf**). Roughness length is determined from **c_sea** and the roughness of the sea surface guides the exchange of momentum, moisture, and heat between ocean and atmosphere. Therefore, an increase in **c_sea** may induce higher magnitude momentum fluxes, modifying low-level atmospheric dynamics, specifically affecting wind speed and heavy precipitation [77, 78]. Differential heating of the land surface causes regional uncertainties which stimulate moist convection by liberating latent heat. The resulting convective cells can grow based on the environmental conditions of atmospheric moisture and vertical instabilities, from non-precipitating clouds to precipitating systems. The rate of the mixing with surrounding air is uncertain and configured by entrainment rates **entr_sc**. Perturbing the **entr_sc** fluctuates the low cloud formation. Thus, a low value for **entr_sc** produces more a low cloud, which steers to reduce incoming short-wave radiation at the surface and thereby leads to lower surface temperature [69, 79-81]. The primary source of uncertainty in microphysics schemes initiates from auto conversion rates of cloud water and ice into precipitating droplets. With the rise in moist air into the higher strata of the atmosphere, adiabatic cooling commences condensation on aerosols and as result water droplets or clouds are formed. Such a process is determined by the parameter **qi0** in COSMO-CLM. A higher concentration for ice auto conversion (**qi0**) leads to increased high cloud cover or reduction in snowfall and finally warms the surface temperature [75, 82, 83]. In the radiation scheme, **uc1** is an important parameter which controls the vertical variation of critical humidity. A reduction of **uc1** increases critical humidity above the boundary layer, which assists in robust mid-level cloud formation. The shrink in cloud cover leads to a cooling surface temperature [75, 84].

6. Discussion

The physical interpretations of the most sensitive parameters and the mechanism influencing the examined variables are explored. Since parameter sensitivity is mostly related to regional conditions, accordingly the results obtained in the present study may not remain valid in other geographical domains. The parameters analyzed in this study are for selective few parameters from the COSMO-CLM, therefore future studies might focus on variation of parameterization schemes as well as initial and boundary conditions. Furthermore, tuning the sensitive parameters using the latest optimization approach can be enforced to improve prediction reliability.

7. Conclusions

In this study, we examined 25 model parameters in extreme weather events observed over the eastern region of India, simulated using COSMO-CLM with various values of model parameters from different physical schemes. The simulated T2M, SLHF, TP, and TCC are compared against reanalysis employing model efficiency metrics presented by Russo et al., (2020) [39]. The primary intention of the paper is to identify the most influencing parameters in the study region by the objective calibration method [38]. Nevertheless, the effect of each parameter on the considered variables for the entire domain and subdomains was measured to scale the extent of model performance. Finally, the paper explains the possibility of improving the model performance against each parameter for the considered variable in the considered domain. The model is distinctly susceptible to a certain group of tested parameters. The scaling factor of the laminar boundary layer for heat (**rlam_heat**) and the ratio of laminar scaling factors for heat over sea and land (**rat_sea**) from the land surface process is sensitive to SLH, and TP. The exponent to get the effective surface area (**e_surf**) from the land surface has a large impact on T2M. Parameters such as cloud ice threshold for auto conversion (**qi0**) from microphysics, mean entrainment rate for shallow convection (**entr_sc**) from convection and parameter for computing the amount of cloud cover in saturated conditions (**uc1**) from radiation play a significant role in producing TP, and TCC fields. The ability of the model worsens from the entire domain to the subdomain against all the variables. The results produced from different subdomains reveal that after choosing distinct parameter values there is an opportunity for the model score to get better. The most significant parameters are **qi0**, **e_surf**, **rlam_heat** and **rat_sea** producing large inconsistencies in model performance over sub-regions. Nevertheless, the same set of parameters does not influence all the variables. A slight dependency by the **fac_rootdp2** from the soil scheme on T2M is evident in this study.

Author Contributions

SB simulated each scenario using the COSMO-CLM model and analyzed the resulting data. IK oversaw the entire project and was also involved in configuring the model. SB and IK collaborated on writing the manuscript and agreed on the final version for publication.

Conflict of Interest

The authors declare no conflict of interest.

Data Availability Statement

All the simulated data and other data sets used for this research and the codes for the post processing model results are available from the corresponding author upon reasonable request.

Funding

This research received no funding.

Acknowledgment

The authors would like to thank Freie Universitat, Berlin for providing computing facilities. The codes and visualizations required for the study were made in R software. The authors would like to thank ECMWF for ERA5 reanalysis data sets. The authors are also particularly grateful to the CLM community for all their efforts in developing COSMO-CLM and making its code available.

References

[1] Pai, D., Nair, S.A., Ramanathan, A., 2013. Long term climatology and trends of heat waves over India during the recent 50 years (1961–2010). Mausam. 64(4), 585–604. DOI: https://doi.org/10.54302/mausam.v64i4.742

[2] Jaswal, A., Rao, P., Singh, V., 2015. Climatology and trends of summer high temperature days in India during 1969–2013. Journal of Earth System Science. 124(1), 1–15.

DOI: https://doi.org/10.1007/s12040-014-0535-8

[3] Rohini, P., Rajeevan, M., Srivastava, A., 2016. On the variability and increasing trends of heat waves over India. Scientific Reports. 6(1), 1–9. DOI: https://doi.org/10.1038/srep26153

[4] Rohini, P., Rajeevan, M., Mukhopadhay, P., 2019. Future projections of heat waves over India from CMIP5 models. Climate Dynamics. 53(1), 975–988. DOI: https://doi.org/10.1007/s00382-019-04700-9

[5] Rajeevan, M., Bhate, J., Jaswal, A.K., 2008. Analysis of variability and trends of extreme rainfall events over India using 104 years of gridded daily rainfall data. Geophysical Research Letters. 35(23). DOI: https://doi.org/10.1029/2008GL035143

[6] De U.S., Dube, R.K., Rao, G.P., 2005. Extreme weather events over India in the last 100 years. Environmental Science, Geography, Economics. 131542400.

[7] Singh, A., Patwardhan, A., 2012. Spatio-temporal distribution of extreme weather events in India. APCBEE Procedia. 1, 258–262. DOI: https://doi.org/10.1016/j.apcbee.2012.03.042

[8] Singh, K., Albert, J., Bhaskaran, P.K., Alam, P., 2021. Assessment of extremely severe cyclonic storms over Bay of Bengal and performance evaluation of ARW model in the prediction of track and intensity. Theoretical and Applied Climatology. 143(3), 1181–1194. DOI: https://doi.org/10.1007/s00704-020-03510-y

[9] Yu, Y., Mainuddin, M., Maniruzzaman, M., et al., 2019. Rainfall and temperature characteristics in the coastal zones of Bangladesh and West Bengal, India. Journal of the Indian Society of Coastal Agricultural Research. 37(2), 12–23.

[10] Cyclone Amphan Led to $14 Billion Economic Losses, Says Global Report [Internet][cited on 2020 Dec 04]. Available from: https://www.hindustantimes.com/india-news/cyclone-amphan-led-to-14-billion-economic-losses-says-global-report/story-FWbYlDCccVSgIDNna93W5L.html

[11] Ahammed, K.B., Pandey, A.C., 2021. Characterization and impact assessment of super cyclonic storm AMPHAN in the Indian subcontinent through space borne observations. Ocean and Coastal Management. 205, 105532. DOI: https://doi.org/10.1016/j.ocecoaman.2021.105532

[12] Majumdar, B., DasGupta, S., 2020. Let Bengal be heard: Dealing with Covid and cyclone amphan together. South Asian History and Culture. 11(3), 317–322. DOI: https://doi.org/10.1080/19472498.2020.1780063

[13] Mishra, A.K., Vanganuru, N., 2020. Monitoring a tropical super cyclone Amphan over Bay of Bengal and nearby region in May 2020. Remote Sensing Applications: Society and Environment. 20, 100408. DOI: https://doi.org/10.1016/j.rsase.2020.100408

[14] Paul, S., Chowdhury S., 2021. Investigation of the character and impact of tropical cyclone Yaas: A study over coastal districts of West Bengal, India. Safety in Extreme Environments. 3, 219–235. DOI: https://doi.org/10.1007/s42797-021-00044-y

[15] Raju, S., Dash, G., Ghosh, S., et al., 2020. Impact of Cyclone Amphan on marine fisheries of West Bengal. Marine Fisheries Information Service Technical and Extension Series No 244, 2020. 244, 30–31.

[16] Sen, S., 2021. Combating tropical cyclones amphan, yaas and after: Eco-restoration of coastal zones. Harvest. 6(1), 33–38.

[17] Singh, K., Albert J., Bhaskaran P.K., et al., 2021. Numerical simulation of an extremely severe cyclonic storm over the Bay of Bengal using WRF modelling system: Influence of model initial condition. Modeling Earth Systems and Environment. 7, 2741–2752. DOI: https://doi.org/10.1007/s40808-020-01069-1

[18] Kumar, A., Singh, D., 2021. Heat stroke-related deaths in India: An analysis of natural causes of deaths, associated with the regional heatwave. Journal of Thermal Biology. 95, 102792. DOI: https://doi.org/10.1016/j.jtherbio.2020.102792

[19] Mahapatra, B., Walia, M., Saggurti, N., 2018.

Extreme weather events induced deaths in India 2001–2014: Trends and differentials by region, sex and age group. Weather and Climate Extremes. 21, 110–116.
DOI: https://doi.org/10.1016/j.wace.2018.08.001

[20] Mishra, V., Kumar, D., Ganguly, A.R., et al., 2014. Reliability of regional and global climate models to simulate precipitation extremes over India. Journal of Geophysical Research: Atmospheres. 119(15), 9301–9323.
DOI: https://doi.org/10.1002/2014JD021636

[21] Ray, K., Giri, R., Ray, S., et al., 2021. An assessment of long-term changes in mortalities due to extreme weather events in India: A study of 50 years' data, 1970–2019. Weather and Climate Extremes. 32, 100315.
DOI: https://doi.org/10.1016/j.wace.2021.100315

[22] Azhar, G.S., Mavalankar, D., Nori-Sarma, A., et al., 2014. Heat-related mortality in India: Excess all-cause mortality associated with the 2010 Ahmedabad heat wave. PLoS One. 9(3), e91831.
DOI: https://doi.org/10.1371/journal.pone.0091831

[23] Dubey, A.K., Kumar, P., 2023. Future projections of heatwave characteristics and dynamics over India using a high-resolution regional earth system model. Climate Dynamics. 60(1–2), 127–145.
DOI: https://doi.org/10.1007/s00382-022-06309-x

[24] Dubey, A.K., Lal ., Kumar, P., et al., 2021. Present and future projections of heatwave hazard-risk over India: A regional earth system model assessment. Environmental Research. 201, 111573.
DOI: https://doi.org/10.1016/j.envres.2021.111573

[25] Bucchignani, E., Montesarchio, M., Cattaneo, L., et al., 2014. Regional climate modeling over China with COSMO-CLM: Performance assessment and climate projections. Journal of Geophysical Research: Atmospheres. 119(21), 12, 151–112, 170.
DOI: https://doi.org/10.1002/2014JD022219

[26] Sørland, S.L., Brogli, R., Pothapakula, P.K., et al., 2021. COSMO-CLM regional climate simulations in the CORDEX framework: A review. Geoscientific Model Development Discussions. 14(8), 5125–5154.
DOI: https://doi.org/10.5194/gmd-14-5125-2021

[27] Singh, S., Mall, R., Dadich, J., et al., 2021. Evaluation of CORDEX-South Asia regional climate models for heat wave simulations over India. Atmospheric Research. 248, 105228.
DOI: https://doi.org/10.1016/j.atmosres.2020.105228

[28] Russo, E., Kirchner, I., Pfahl, S., et al., 2019. Sensitivity studies with the regional climate model COSMO-CLM 5.0 over the CORDEX Central Asia Domain. Geoscientific Model Development. 12(12), 5229–5249.
DOI: https://doi.org/10.5194/gmd-12-5229-2019

[29] Zhou, W., Tang, J., Wang, X., et al., 2016. Evaluation of regional climate simulations over the CORDEX-EA-II domain using the COSMO-CLM model. Asia-Pacific Journal of Atmospheric Sciences. 52(2), 107–127.

[30] Wang, D., Menz, C., Simon, T., et al., 2013. Regional dynamical downscaling with CCLM over East Asia. Meteorology and Atmospheric Physics. 121(1), 39–53.
DOI: https://doi.org/10.1007/s00703-013-0250-z

[31] Hourdin, F., Mauritsen, T., Gettelman, A., et al., 2017. The art and science of climate model tuning. Bulletin of the American Meteorological Society. 98(3), 589–602.
DOI: https://doi.org/10.1175/BAMS-D-15-00135.1

[32] Knutti, R., Stocker, T.F., Joos, F., et al., 2002. Constraints on radiative forcing and future climate change from observations and climate model ensembles. Nature. 416, 719–723.
DOI: https://doi.org/10.1038/416719a

[33] Voudouri, A., Khain, P., Carmona, I., et al., 2017. Objective calibration of numerical weather prediction models. Atmospheric Research. 190, 128–140.
DOI: https://doi.org/10.1016/j.atmosres.2017.02.007

[34] Bucchignani, E., Cattaneo, L., Panitz, H.J., et al., 2016. Sensitivity analysis with the regional

climate model COSMO-CLM over the CORDEX-MENA domain. Meteorology and Atmospheric Physics. 128(1), 73–95.
DOI: https://doi.org/10.1007/s00703-015-0403-3

[35] Bellprat, O., Kotlarski, S., Lüthi, D., et al., 2016. Objective calibration of regional climate models: Application over Europe and North America. Journal of Climate. 29(2), 819–838.
DOI: https://doi.org/10.1175/JCLI-D-15-0302.1

[36] Bhatla, R., Verma, S., Ghosh, S., et al., 2020. Performance of regional climate model in simulating Indian summer monsoon over Indian homogeneous region. Theoretical and Applied Climatology. 139(3), 1121–1135.
DOI: https://doi.org/10.1007/s00704-019-03045-x

[37] Annan, J., Hargreaves, J., 2007. Efficient estimation and ensemble generation in climate modelling. Philosophical Transactions of the Royal Society A: Mathematical, Physical and Engineering Sciences. 365(1857), 2077–2088.
DOI: https://doi.org/10.1098/rsta.2007.2067

[38] Bellprat, O., Kotlarski, S., Lüthi, D., et al., 2012. Objective calibration of regional climate models. Journal of Geophysical Research: Atmospheres. 117(D23).
DOI: https://doi.org/10.1029/2012JD018262

[39] Russo E., Sørland S.L., Kirchner I., et al., 2020. Exploring the parameter space of the COSMO-CLM v5.0 regional climate model for the Central Asia CORDEX domain. Geoscientific Model Development. 13(11), 5779–5797.
DOI: https://gmd.copernicus.org/articles/13/5779/2020/

[40] Bellprat, O., Kotlarski, S., Lüthi, D., et al., 2012. Exploring perturbed physics ensembles in a regional climate model. Journal of Climate. 25(13), 4582–4599.

[41] Neelin, J.D., Bracco, A., Luo, H., et al., 2010. Considerations for parameter optimization and sensitivity in climate models. Proceedings of the National Academy of Sciences. 107(50), 21349–21354.

[42] Adinolfi, M., Raffa, M., Reder, A., et al., 2021. Evaluation and expected changes of summer precipitation at convection permitting scale with COSMO-CLM over alpine space. Atmosphere. 12(1), 54.
DOI: https://doi.org/10.3390/atmos12010054

[43] Ahrens, B., Dobler, A., 2010. Analysis of the Indian summer monsoon system in the regional climate model COSMO-CLM. EGU General Assembly Conference Abstracts. 115(D16).
DOI: https://doi.org/10.1029/2009JD013497

[44] Ahrens, B., Meier T., Brisson, E., 2020. Diurnal cycle of precipitation in the himalayan foothills–observations and model results. Himalayan Weather and Climate and their Impact on the Environment. 73–89.
DOI: https://doi.org/10.1007/978-3-030-29684-1_5

[45] Bucchignani, E., Montesarchio, M., Zollo, A.L., et al., 2016. High-resolution climate simulations with COSMO-CLM over Italy: Performance evaluation and climate projections for the 21st century. International Journal of Climatology. 36(2), 735–756.
DOI: https://doi.org/10.1002/joc.4379

[46] Di, Z., Duan, Q., Gong, W., et al., 2015. Assessing WRF model parameter sensitivity: A case study with 5 day summer precipitation forecasting in the Greater Beijing Area. Geophysical Research Letters. 42(2), 579–587.
DOI: https://doi.org/10.1002/2014GL061623

[47] Quan, J., Di, Z., Duan, Q., et al., 2016. An evaluation of parametric sensitivities of different meteorological variables simulated by the WRF model. Quarterly Journal of the Royal Meteorological Society. 142(700), 2925–2934.
DOI: https://doi.org/10.1002/qj.2885

[48] Chinta, S., Yaswanth Sai, J., Balaji, C., 2021. Assessment of WRF model parameter sensitivity for high-intensity precipitation events during the Indian summer monsoon. Earth and Space Science. 8(6), e2020EA001471.
DOI: https://doi.org/10.1029/2020EA001471

[49] Rockel, B., Geyer, B., 2008. The performance of the regional climate model CLM in different climate regions, based on the example of precipitation. Meteorologische Zeitschrift. 17(4),

487–498.
DOI: https://doi.org/10.1127/0941-2948/2008/0297

[50] Rockel, B., Will, A., Hense, A., 2008. The regional climate model COSMO-CLM (CCLM). Meteorologische Zeitschrift. 17(4), 347–348.
DOI: https://doi.org/10.1127/0941-2948/2008/0309

[51] Schättler, U., Doms, G., Schraff, C., 2008. A description of the nonhydrostatic regional COSMO-model part VII: User's guide. Deutscher Wetterdienst: Offenbach, Germany.

[52] Doms, D., Förstner, J., Heise, E., et al., 2011. A description of the nonhydrostatic regional COSMO-model, Part II: Physical parameterization. Deutscher Wetterdienst: Offenbach, Germany.

[53] Dee, D.P., Uppala, S.M., Simmons, A., et al., 2011. The ERA-Interim reanalysis: configuration and performance of the data assimilation system. Quarterly Journal of the Royal Meteorological Society. 137(656), 553–597.
DOI: https://doi.org/10.1002/qj.828

[54] Tiedtke, M., 1989. A comprehensive mass flux scheme for cumulus parameterization in large-scale models. Monthly Weather Review. 117(8), 1779–1800.
DOI: https://doi.org/10.1175/1520-0493(1989)117<1779:ACMFSF>2.0.CO;2

[55] Tegen, I., Hollrig, P., Chin, M., et al., 1997. Contribution of different aerosol species to the global aerosol extinction optical thickness: Estimates from model results. Journal of Geophysical Research: Atmospheres. 102(D20), 23895–23915.
DOI: https://doi.org/10.1029/97JD01864

[56] Asharaf, S., Ahrens, B., 2013. Soil-moisture memory in the regional climate model COSMO-CLM during the Indian summer monsoon season. Journal of Geophysical Research: Atmospheres. 118(12), 6144–6151.
DOI: https://doi.org/10.1002/jgrd.50429

[57] Dobler, A., Ahrens, B., 2011. Four climate change scenarios for the Indian summer monsoon by the regional climate model COSMO-CLM. Journal of Geophysical Research: Atmospheres. 116(D24).
DOI: https://doi.org/10.1029/2011JD016329

[58] Fallah, B., Russo, E., Acevedo, W., et al., 2018. Towards high-resolution climate reconstruction using an off-line data assimilation and COSMO-CLM 5.00 model. Climate of the Past. 14(9), 1345–1360.
DOI: https://doi.org/10.5194/cp-14-1345-2018

[59] Huang, J., Wang, Y., Fischer, T., et al., 2017. Simulation and projection of climatic changes in the Indus River Basin, using the regional climate model COSMO-CLM. International Journal of Climatology. 37(5), 2545–2562.
DOI: https://doi.org/10.1002/joc.4864

[60] Platonov, V., Varentsov, M., 2021. Introducing a new detailed long-term COSMO-CLM hindcast for the Russian arctic and the first results of its evaluation. Atmosphere. 12(3), 350.
DOI: https://doi.org/10.3390/atmos12030350

[61] Cherubini, F., Huang, B., Hu, X., et al., 2018. Quantifying the climate response to extreme land cover changes in Europe with a regional model. Environmental Research Letters. 13(7), 074002.
DOI: https://doi.org/10.1088/1748-9326/aac794

[62] Asis, M., Saon, B., Monotosh Das, B., et al., 2016.Extreme weather events and trends of climatic variable in West Bengal: analysis and occurrence. AICPAM-NICRA (Mohanpur Centre): Kalyani, Nadia.

[63] Hersbach, H., Bell, B., Berrisford, P., et al., 2020. The ERA5 global reanalysis. Quarterly Journal of the Royal Meteorological Society. 146(730), 1999–2049.
DOI: https://doi.org/10.1002/qj.3803

[64] Hoffmann, L., Günther, G., Li, D., et al., 2019. From ERA-Interim to ERA5: the considerable impact of ECMWF's next-generation reanalysis on Lagrangian transport simulations. Atmospheric Chemistry and Physics. 19(5), 3097–3124.
DOI: https://doi.org/10.5194/acp-19-3097-2019

[65] Mahto, S.S., Mishra, V., 2019. Does ERA-5 outperform other reanalysis products for

hydrologic applications in India? Journal of Geophysical Research: Atmospheres. 124(16), 9423–9441.
DOI: https://doi.org/10.1029/2019JD031155

[66] Huffman GJ, Bolvin DT, Nelkin EJ, Tan J. Integrated Multi-satellitE Retrievals for GPM (IMERG) technical documentation. Nasa/Gsfc Code 2015; 612(47):2019.

[67] Murphy, A.H., 1988. Skill scores based on the mean square error and their relationships to the correlation coefficient. Monthly Weather Review. 116(12), 2417–2424.
DOI: https://doi.org/10.1175/1520-0493(1988)116<2417:SSBOTM>2.0.CO;2

[68] Murphy, J.M., Booth, B.B., Collins, M., et al., 2007. A methodology for probabilistic predictions of regional climate change from perturbed physics ensembles. Philosophical Transactions of the Royal Society A: Mathematical, Physical and Engineering Sciences. 365(1857), 1993–2028.
DOI: https://doi.org/10.1098/rsta.2007.2077

[69] Murphy, J.M., Sexton, D.M., Barnett, D.N., et al., 2004. Quantification of modelling uncertainties in a large ensemble of climate change simulations. Nature. 430(7001), 768–772.
DOI: https://doi.org/10.1038/nature02771

[70] Wilks, D.S., 2011. Statistical methods in the atmospheric sciences. Elsevier: Berkeley, CA.
DOI: https://doi.org/10.1016/C2017-0-03921-6

[71] Baki, H., Chinta, S., Balaji, C., et al., 2021. Determining the sensitive parameters of WRF model for the prediction of tropical cyclones in the Bay of Bengal using global sensitivity analysis and machine learning. Geoscientific Model Development Discussions. 1–46.

[72] Baki, H., Chinta, S., Balaji, C., et al., 2021. A sensitivity study of WRF model microphysics and cumulus parameterization schemes for the simulation of tropical cyclones using GPM radar data. Journal of Earth System Scien. 130, 4, 1–30.

[73] Chinta, S., Balaji, C., 2020. Calibration of WRF model parameters using multiobjective adaptive surrogate model-based optimization to improve the prediction of the Indian summer monsoon. Climate Dynamics. 55, 3, 631–650.

[74] Cerenzia, I., Tampieri, F., Tesini, M.S., 2014. Diagnosis of turbulence schema in stable atmospheric conditions and sensitivity tests. Cosmo Newsletter. 14, 1–11.

[75] Bellprat, O., 2013. Parameter uncertainty and calibration of regional climate models [PhD thesis]. Zürich: ETH Zurich.

[76] Voudouri, A., Khain, P., Carmona, I., et al., 2018. Optimization of high resolution COSMO model performance over Switzerland and Northern Italy. Atmospheric Research. 213, 70–85.
DOI: https://doi.org/10.1016/j.atmosres.2018.05.026

[77] Thévenot, O., Bouin, M.N., Ducrocq, V., et al., 2016. Influence of the sea state on Mediterranean heavy precipitation: A case-study from HyMeX SOP1. Quarterly Journal of the Royal Meteorological Society. 142, 377–389.
DOI: https://doi.org/10.1002/qj.2660

[78] Carlsson, B., Papadimitrakis, Y., Rutgersson, A., 2010. Evaluation of a roughness length model and sea surface properties with data from the Baltic Sea. Journal of Physical Oceanography. 40(9), 2007–2024.
DOI: https://doi.org/10.1175/2010JPO4340.1

[79] Rougier, J., Sexton, D.M., Murphy, J.M., et al., 2009. Analyzing the climate sensitivity of the HadSM3 climate model using ensembles from different but related experiments. Journal of Climate. 22(13), 3540–3557.
DOI: https://doi.org/10.1175/2008JCLI2533.1

[80] Klocke, D., Pincus, R., Quaas, J., 2011. On constraining estimates of climate sensitivity with present-day observations through model weighting. Journal of Climate. 24(23), 6092–6099.
DOI: https://doi.org/10.1175/2011JCLI4193.1

[81] Buzzi, M., Rotach, M., Raschendorfer, M., et al., 2011. Evaluation of the COSMO-SC turbulence scheme in a shear-driven stable boundary

layer. Meteorologische Zeitschrift (Berlin). 20(3), 335–350.
DOI: https://doi.org/10.1127/0941-2948/2011/0050

[82] Bachner, S., Kapala, A., Simmer, C., 2008. Evaluation of daily precipitation characteristics in the CLM and their sensitivity to parameterizations. Meteorologische Zeitschrift. 17(4), 407–419.
DOI: https://doi.org/10.1127/0941-2948/2008/0300

[83] Zhao, Q., Carr, F.H., 1997. A prognostic cloud scheme for operational NWP models. Monthly Weather Review. 125(8), 1931–1953.
DOI: https://doi.org/10.1175/1520-0493(1997)125<1931:APCSFO>2.0.CO;2

[84] Zhu, P., Zuidema, P., 2009. On the use of PDF schemes to parameterize sub-grid clouds. Geophysical Research Letters. 36(5).
DOI: https://doi.org/10.1029/2008GL036817